Shallow Stratification of the Northern Oceans: An Evaluation of the Nine Analyses

James Carton and Gennady Chepurin (Univ. MD) , and You-Soon Chang (GFDL)

Introduction

This paper explores the mean state and variability of upper ocean water properties in the northern and tropical oceans during the years 1962-2001 as represented in nine ocean analyses. Indications of decadal changes in upper ocean water masses have been seen many parts of the ocean (e.g. *Lazier, 1995; Joyce and Robbins, 1996; McPhaden and Zhang, 2002*). Here we apply a set of nine ocean analyses spanning part or all of the period 1962-2001 to examination of changes in the stratification of the upper layers of northern and tropical oceans. Our goals are to explore representation of key subseasonal changes in water masses in different analyses, and suggest possible causes of differences in representation as a way of understanding the uncertainty in the analysis estimates.

Table 1 Analyses considered in this study. The vertical resolution given below only includes the number of levels between the surface and 700m. UK-FOAM has been shortened from 2004 to 1998 because of some problems at the end of the analysis period.

Analysis	Time Span	Surface fluxes			Model, res.	Analysis procedure
		Moment.	Heat	Fresh water		
CERFACS *Davey* (2005)	1962-2001	ERA-40 Reanal	ERA 40 Reanal	ERA-40 corrected in tropics	ORCA2 vers. OPA 2°x2°-1/2° 31 lev	Sequential
ECMWF *Balmaseda et al. (2007)*	1962-2001	ERA-40 Reanal	ERA 40 Reanal	ERA-40 corrected in tropics	HOPE 2°x2°-1/2° 21 lev	Sequential
GECCO *Köhl and Stammer (2008)*	1950-1999	NCEP Reanal	NCEP Reanal	NCEP Reanal	MITGCM 1°x1° 23 lev	4DVar
GFDL *Zhang et al. (2008)*	1979-2002	Coupled	Coupled	Coupled	MOM4 1°x1°-1/3° 32 lev	Sequential
GODAS *Behringer* (2005)	1979-2005	NCEP Reanal.-2	NCEP Reanal.-2	NCEP Reanal.-2	MOM3 1°x1°-1/3° 40 lev	Sequential
INGV Bellucci, *et al. (2007)*	1962-2001	ERA-40 Reanal	ERA 40 Reanal	ERA-40 corrected in tropics	OPA 2°x2°-1/2° 31 lev	Sequential
SODA *Carton and Giese* (2008)	1958-2005	ERA-40 Reanal	bulk heat flux	GPCP rain	POP2.1 1/4°x1/4° 40 lev	Sequential
UK-FOAM *Bell. (2000), Bell et al. (2004)*	1962-1998	ERA-40 Reanal	ERA 40 Reanal	ERA-40 corrected in tropics	GloSea 1°x1°-1/3° 20 lev	Sequential
UK-OI *Ingleby and Huddleston (2007)*	1962-2001				1°x1°	Objective Analysis

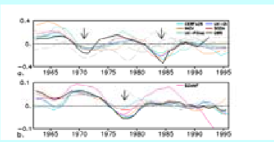

Figure 9 Annually averaged salinity anomaly from the 1962-1995 average, averaged horizontally and vertically in two regions. **a)** Labrador Sea (53°W-59°W, 50°N-56°N) averaged vertically (0-250m). Observations (black solid) are from *Lazier, 1995*). Two 'Great Salinity Anomaly' decreases are apparent 1967-1971 and again 1978-1985 (see *Lazier, 1995* for discussion). **b)** Norwegian Basin (0-5°E, 63°N-69°N) averaged vertically (0-500m). The Great Salinity Anomaly which appeared in the Labrador Sea in early 1970s appears at this location in the late 1970s (see *Nilsen and Falck, 2003* for

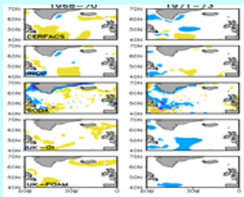

Figure 10 Salinity anomaly from the 1962-1995 average, averaged vertically (0-250m) and in time for three 3-year periods 1968-70 and 1971-3 for the analyses shown in color in **Fig. 9a**. The first two periods show early and mid stages of the 1970s Great Salinity Anomaly, while the third period shows the mid-stage of the 1980s Great Salinity Anomaly**.**

Five analyses; CERFACS, INGV, SODA, UK-FOAM, and UK-OI; show pronounced freshening events consistent with the observed record in both the Labrador Sea and the Norwegian Basin. The analysis with the highest spatial resolution, SODA, shows the most distinct advection of freshwater along the East and West Greenland Currents into the Labrador Sea.

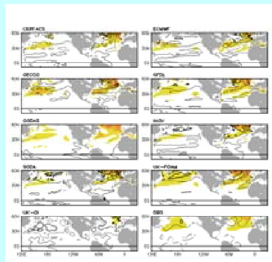

Figure 1a Winter-spring (JFM) mixed layer depth during the 16 year interval 1980-1995 computed using a 0.2°C absolute temperature criterion (colors in meters). Also shown is the difference between this depth and the depth of the mixed layer computed using an equivalent density criterion. Positive values of this difference indicate the thickness of a salinity barrier layer, while negative values indicate the thickness of a layer of temperature and salinity compensation (contours at ±10, ±30m, negative contours are dashed). Observations are from H. Liu *(personal communication, 2008)*.

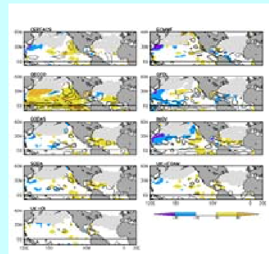

Figure 2 Time mean difference between analysis and observation properties of the 25.5σ surface of the depth computed during the 16-year period 1980-1995. Depth difference is shown in color (m) and salinity difference in contours (±0.1, ±0.3psu, negative contours are dashed). Grey areas define seasonal outcropping regions.

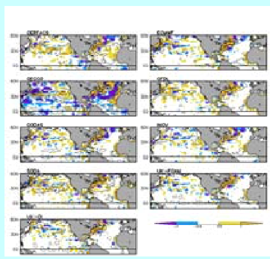

Figure 1b Winter-spring (JFM) SST difference (°C, analysis minus observation) computed during the 16 year interval 1980-1995. Colors show difference between the uppermost analysis level and a corresponding observation. Contours show the difference between the uppermost analysis level and the HADSST bulk SST analysis (contours at ±0.25 and ±1°C, negative contours dashed).

The seasonal behavior of SST and mixed layer properties in the sequential and 4DVar analyses is qualitatively consistent with observations. The single no-model analysis, UK-OI, has very shallow mixed layers even in winter due to the presence of a shallow temperature inversion. In a couple of analyses anomalously cool winter-spring North Atlantic SSTs appear to allow the mixed layer in excessively large geographic regions to deepen into the layer containing North Atlantic Subtropical Mode Water. The mean properties of upper ocean constant density surfaces such as the 25.5 and 26.5σ surfaces are qualitatively correct for the sequential analyses and the no-model analysis although most show a <10m anomalous deepening in the eastern North Pacific and a similar shallowing in the west. The GECCO 4DVar analysis shows a 10-30m basin-wide deepening of these isopycnal surfaces in the North Pacific in the 1990s.

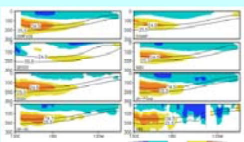

Figure 6 Change in density (kg m^{-3}) averaged 1990-1999 minus 1970-1977 along the equator in the Pacific as a function of depth. Depth of the mean 24.5σ and 25.5σ surfaces are superimposed.

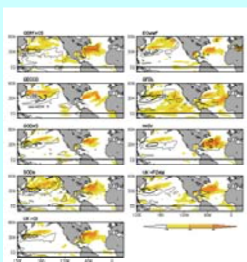

Figure 3 Root-mean-square variability of the depth of constant density surfaces (3-yr low pass filtered) computed over the full analysis period. Colors show the RMS depth of the 26.5σ surface. Contours show the RMS depth of the 25.5σ surface (contour interval is 10m, 20m contour is bold).

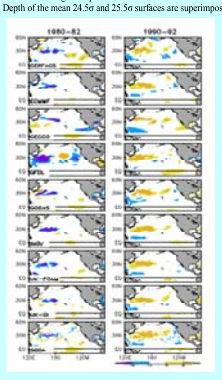

Figure 4 Depth anomaly (m) of the 25.5σ surface relative to the 1980-1995 average for two 3-year periods, 1980-82 and 1990-92 (following *Miller and Schneider, 2000*), when the decadal cycle of North Pacific variability was in opposite phases.

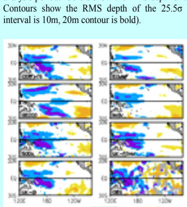

Figure 5 Change in depth (m) of the 25.5σ surface averaged 1990-1999 minus 1970-1977. Observations (lower right) show a deepening in the east and a shallowing in the west (see *McPhaden and Zhang, 2002* for discussion). Grey regions indicate limited CTD and station sampling.

For most analyses the 25.5σ and 26.5σ isopycnal surfaces depth variability is mainly confined to regions of mode water mass formation and adjacent subtropical gyres. In the subtropical North Pacific a major component of this variability is the result of a succession of density anomalies formed in the northern North Pacific which travel clockwise around the subtropical gyre as previously described by *Miller and Schneider (2000)*. These anomalies are represented in a qualitatively similar way in all analyses.The 25.5σ surface in the North Pacific also shows a reduction in its zonal tilt between the 1970s and 1990s as the result of a deepening of the pycnocline in the east and a shallowing of the pycnocline in the west.This reduction in zonal tilt and associated reduction in vertical shear of meridional velocity *McPhaden and Zhang (2002)* associate with a slowing down of the shallow meridional overturning circulation.The sequential analyses generally show this change of slope extending to the equator, but the GECCO 4DVar analysis does not.The one analysis using a form of coupled assimilation, GFDL, shows significant multi-decadal near-surface freshening trends in some locations that do not appear in the other analyses.

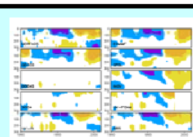

Figure 7 Salinity anomalies from the 1990-2001 average with depth averaged horizontally in a 2°x2° box centered on the location of the Hawaii Ocean Time Series (23°N, 158°W) and in time with a 6-month running filter. Observations (lower right) show a fresh and then salty anomaly appearing first at the surface and then extending into the water column to 200m depth (see *Lukas, 2002* for discussion).

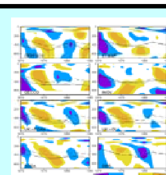

Figure 8 Potential vorticity anomaly (normalized by PV variability at each level) from the 1970-1985 average, averaged in a 2°x2° box centered on the location of Station S (32°N, 64°W) and in time with an annual filter. Solid line indicates depth of the 26.5σ surface in each analysis. Observations (lower right) show a succession of high and low potential vorticity events (see *Joyce and Robbins, 1996* for discussion).

The records of two time series, the Hawaii Ocean Time series in the North Pacific subtropical gyre and the Station S time series in the North Atlantic subtropical gyre are used to examine the response of the analyses to year-to-year changes in surface fluxes in the subtropics. In the North Pacific *Lukas (2001)* identifies a low salinity event spanning the years 1995-7. Comparison of the analyses at this location shows that most are able to reproduce this feature. Two analyses, SODA and GODAS, had weak anomalies as a result, we believe, of analysis procedures which limit variability of salinity in the presence of many temperature observations. In the North Atlantic all analyses are able to reproduce a reduction in North Atlantic Subtropical Mode Water thickness which occurred in the mid-1970s. However, the far field geographic representation of both the Pacific and Atlantic anomalies vary among the analyses.